



| | |
|--------------|---|
| Title | Fundamental Study for the Relationship between Melt Flow and Spatter in High-Power Laser Welding of Pure Titanium |
| Author(s) | Kawahito, Yousuke; Katayama, Seiji; Nakamura, Hiroshi |
| Citation | Transactions of JWRI. 2015, 44(2), p. 27-32 |
| Version Type | VoR |
| URL | https://doi.org/10.18910/57270 |
| rights | |
| Note | |

The University of Osaka Institutional Knowledge Archive : OUKA

<https://ir.library.osaka-u.ac.jp/>

The University of Osaka

Fundamental Study for the Relationship between Melt Flow and Spatter in High-Power Laser Welding of Pure Titanium[†]

NAKAMURA Hiroshi *, KAWAHITO Yousuke **, KATAYAMA Seiji ***

Abstract

The objectives of this study is to clarify the relationship between melt flow and spatters ejected from a molten pool during 10 kW laser welding of a pure titanium plate. Three-dimensional X-ray transmission in-situ observation of the weld molten pool with tungsten carbide tracers revealed that the melt flowed mainly along the bottom of the molten pool from the keyhole tip to the rear part and then from the rear to the front near the surface of the molten pool, while the melt in front of a keyhole flowed upwards along the keyhole wall at a velocity of less than 0.6 m/s and then was accelerated to 2.1 m/s at the height of about 2 mm above the keyhole inlet. One-way upward melt flows were continuously piled up at the tip of the elongated melt, resulting in spattering as droplets from the molten pool. Moreover, about 80 % of spatters were generated from melts of the front or sides of the keyhole at the speeds of less than 50 mm/s. When the welding speed increased from 50 - 100 mm/s to 300 mm/s, the ratio and the size of spatters occurring from the rear part of a keyhole increased from 20% to 80 % and became smaller than 1 mm.

KEY WORDS: (Laser welding), (Melt flow), (Spatter), (Pure titanium), (X-ray transmission observation)

1. Introduction

Welding is a fundamental technology for joining metals in manufacturing. Clarification of melt flow behavior in a molten pool during welding is essential for production of a high-quality weld without defects. Some welding defects such as porosity and underfilling occur under the improper conditions of low welding speeds and extremely high welding speeds, and degrade the mechanical properties of the welded joints. Spatters causing underfilled weld beads are formed by the ejection of melt droplets from the molten pool. Underfilling, which is the concavity of the weld bead surface, sometimes decreases the mechanical properties of welds. Porosity is a cavity, a pore or a blowhole in the weld metal after solidification, and large-sized pores reduce the mechanical properties. In particular, some papers have reported the formation mechanism of spatters resulting in the underfill¹⁾⁻⁷⁾. The formation mechanism of spatters has been discussed in terms of the relationship between spattering and molten pool behavior¹⁾. Qualitative melt flows during laser welding of stainless steel were described, but quantitative study of melt flows has not been performed. Also, spattering during laser welding of titanium has not been treated.

In this paper, therefore, high power laser welding for thick plates of pure titanium was performed to investigate

the formation mechanisms of spatters from a molten metal. To understand the three-dimensional melt flows and the calculated melt flow velocity in the molten pool, two X-ray transmission in-situ direct observation systems were utilized.

2. Material Used and Experimental procedures

The material used is commercially available pure titanium, whose chemical compositions are shown in **Table 1**. The content of oxygen (O) is about 0.1 mass%, and those of the other impurity elements are extremely small.

The experimental setup for observation of melt flows inside the molten pool, keyhole behavior, plume ejection, bubbles/porosity formation and spatters generation during high power disk laser welding is schematically shown in **Fig. 1**. A continuous wave (CW) high power disk laser with a maximum power of 16 kW and a wavelength of 1030 nm was used. A laser beam with a beam parameter product (BPP) of 8 mm*mrad was transmitted via an optical fiber of 200 μm in core diameter. The laser beam diameter at the focal point was approximately 280 μm , achieving high brightness.

Fig. 2 shows laser-related parameters such as laser beam focusing dimensions, laser power density

[†] Received on November **, 2015

* Graduate Student

** Associate Professor

*** Professor

Transactions of JWRI is published by Joining and Welding Research Institute, Osaka University, Ibaraki, Osaka 567-0047, Japan

Fundamental Study for Relationship of Melt Flows and Spatters in High Power Laser Welding of Pure Titanium

Table 1 Chemical compositions of pure titanium used.

| Chemical compositions (mass%) | | | | | |
|-------------------------------|------|------|------|-------|------|
| C | Fe | N | O | H | Ti |
| 0.00 | 0.04 | 0.00 | 0.11 | 0.001 | Bal. |

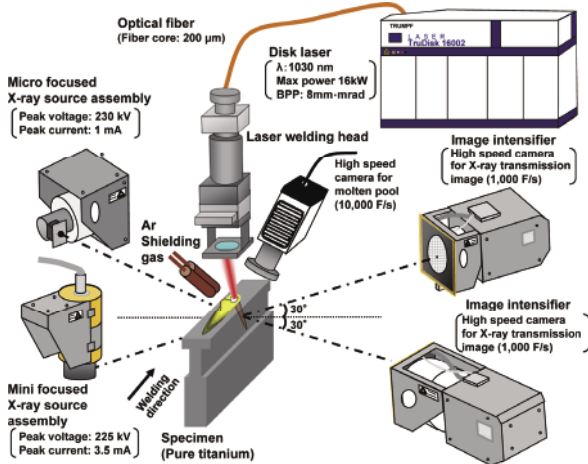


Fig. 1 Schematic experimental setup for observing melt flows inside molten pool and spatters generation during high power disk laser welding of pure titanium plate.

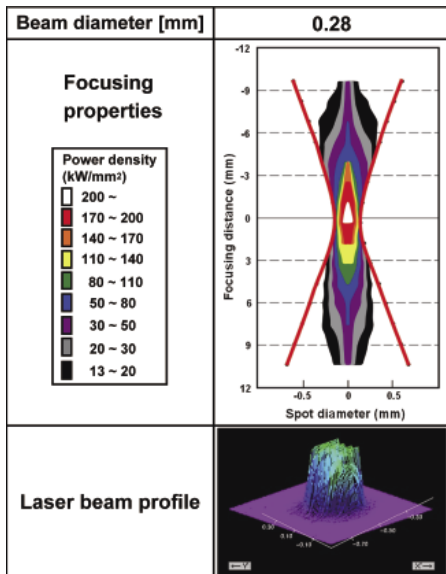


Fig. 2 Focusing dimensions of laser beam, laser power density distribution, laser beam diameter and laser beam profile at focal point.

distribution, and a laser beam diameter and a laser beam profile at the focal point. Here, the beam diameter is defined at a spot size containing 86 % energy of a 4 kW incident laser power, and laser power density (kW/mm²) is calculated and indicated at a power of 10 kW. The laser head was inclined at an incident angle (θ) of 20° forward to avoid being affected by a reflection back into the laser.

Laser welding was performed at 10 kW constant power and various speeds on the focal position of 0 mm above the specimen surface. To suppress the oxidation of the molten titanium surface, an argon shielding gas was supplied at a flow rate of 50 l/min from two gas nozzles of 16 mm in inner diameter.

Spatter behavior was observed at 10,000 frames/s with a high-speed video camera. To clarify the relationship between melt flows inside the molten pool and spatter formation within the molten pool and near the front wall of the keyhole, two or three-dimensional X-ray transmission in-situ direct observation system were employed. With the three-dimensional X-ray transmission in-situ direct observation system, spatter formation phenomena around the keyhole inlet were observed from different stereoscopic directions at 1,000 frames/s utilizing two sources: (1) a micro focused X-ray source with a peak voltage of 230 kV and a peak current of 1 mA, and (2) a mini focused X-ray source with a peak voltage of 225 kV and a peak current of 3.5 mA. Thus, the observation results could be displayed three-dimensionally. A T-shaped specimen with WC particles of about 0.5 mm diameter was prepared for investigating melt flows in the molten pool and around a keyhole during laser welding.

3. Experimental Results and Discussion

3.1 Formation of weld beads and spatters in high power laser welding of pure titanium

Laser melt run (bead-on-plate) welding was performed on titanium plates of 10 and 20 mm in thickness at a power of 10 kW and welding speeds of 17, 50, 100, 200 and 300 mm/s. Examples of typical surface appearances and cross sections of laser weld beads produced are shown together with the data of bead widths and penetrations in **Fig. 3**. The width and penetration of the laser weld beads became narrower and shallower with an increase in the welding speed, respectively. The photos show that underfilled weld beads with spatters were formed at all welding speeds. At the lower speeds of 17 and 50 mm/s, spatters of more than 1 mm in diameter were formed. At above 100 mm/s, the spatters adhering to the bead surface were smaller than the size of 1 mm. It was also recognized that in a wide range of laser welding conditions, spatters were generated more easily in titanium than in stainless steel⁶⁾.

In order to understand the formation tendency of spatters depending upon respective welding speeds, the behavior of the molten pool surface around a keyhole, resulting in the formation of spatters, was observed by high-speed video observation. Typical images of high-speed video and their schematic illustrations of the molten pool around the keyhole during laser welding at 17 mm/s are shown in **Fig. 4**. It exhibits the formation process of a spatter. Here, 0 s indicates the initiation time of laser irradiation. Molten metal around the keyhole inlet was elongated upwardly, and the elongated molten metal around the keyhole inlet became droplets. Such flying droplets and the resultant solid particles spread on the

| Welding speed | 17 mm/s | 50 mm/s | 100 mm/s | 200 mm/s | 300 mm/s |
|---------------|---------|---------|----------|----------|----------|
| Bead surface | | | | | |
| 5 mm I | | | | | |
| Cross section | | | | | |
| 3 mm I | | | | | |
| Bead width | 9.7 mm | 4.2 mm | 3.2 mm | 2.0 mm | 1.6 mm |
| Penetration | 10.3 mm | 7.5 mm | 6.0 mm | 4.0 mm | 3.1 mm |

Fig. 3 Surface appearances and cross sections, bead widths and penetration depths of laser weld beads in pure Ti plate.

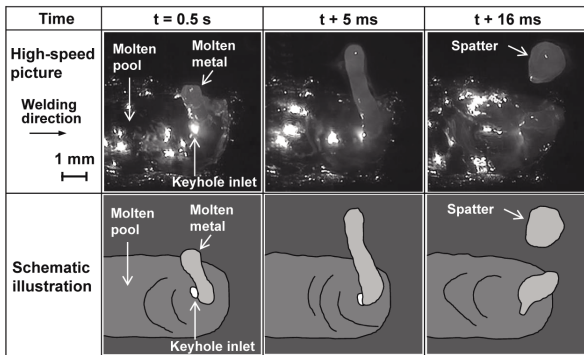


Fig. 4 High-speed images of spattering with schematic illustration of spatter formation during disk laser welding of Ti plate at 10 kW power and 17 mm/s welding speed.

plate are both called spatters. It was frequently observed that the molten metal in front of a keyhole was elongated to become droplets.

Subsequently, the generation locations and sizes of spatters were investigated. **Fig. 5** shows typical images of spattering and their schematic illustrations of the molten pool around the keyhole during laser welding at 17, 100 and 300 mm/s. It is observed that the elongation of molten metal occurred from the front, side and rear parts of a keyhole at 17, 100 and 300 mm/s, respectively. It suggests that the locations of spatter generation is different at different welding speeds. Therefore, 50 spatters formed at respective welding speeds were classified into 3 locations: keyhole front, keyhole sides and keyhole rear to the welding direction, and the spatter was divided into larger or smaller types of over or below 1 mm diameter. The measured results are shown in **Fig. 6**. At the lower speeds of 17 and 50 mm/s, about 80% of the elongated molten metal occurred from the keyhole front and side. At 100 mm/s, the elongation of molten metal from the keyhole sides was dominant. At 300 mm/s, spatter was generated mainly from the keyhole rear. At over 50 mm/s, spatter from the keyhole front decreased but spatter from the keyhole rear increased with an increase in the welding speed. Larger sizes of spatter was formed at lower welding speeds, and the number of large-sized spatter decreased with increasing the welding speed.

From such observation results, it was found that the large-sized spatter was likely to occur at low welding speeds, and that about 80 % of spatter was generated

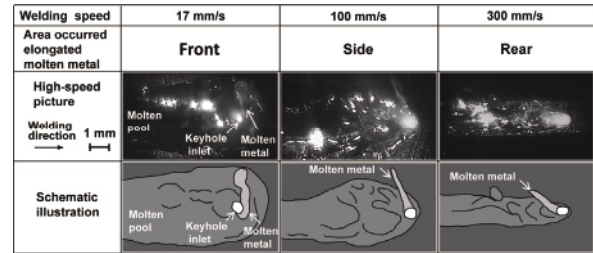


Fig. 5 Typical examples of high speed observation pictures of molten pool and elongated molten metal during laser welding at three speeds, showing formation locations of spatters from molten metal around keyhole inlet.

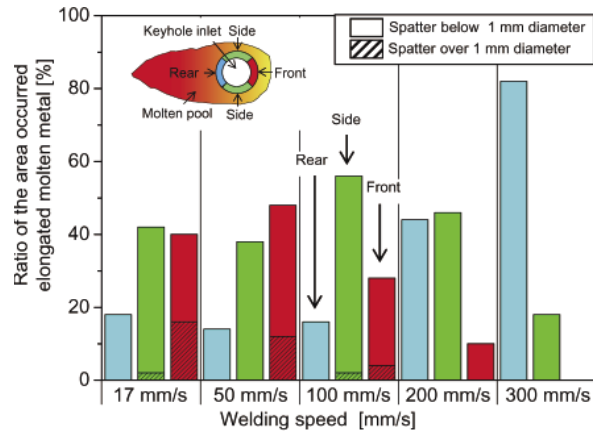


Fig. 6 Effect of welding speed on occurrence locations and sizes of spatters.

from the keyhole front or sides at the welding speeds of less than 50 mm/s. But the ratio of spatter formation from the keyhole rear increased from 20 to 80 % with an increase in the welding speed from 100 to 300 mm/s.

The former paper⁶⁾ reported that spatters generated from the rear part of a keyhole inlet were suppressed during laser welding of austenitic stainless steel when a laser beam was tilted at 20° forward in the welding direction. In this research of laser welding of titanium, the forward tilt angle of 20° was adopted. Nevertheless, spatter was still formed during low and high welding speeds of titanium. It is consequently judged that spatter was more liable to occur in titanium than in stainless steel.

3.2 Three dimensional melt flow in molten pool at high power laser welding

In order to understand spatter formation and laser welding phenomena in detail, melt flows in the molten pool and keyhole behavior were observed during laser welding of titanium plate at 10 kW and 17 mm/s through an X-ray transmission in-situ observation system. Observation results of melt flows are shown in **Fig. 7**. Here, a Platinum (Pt) wire of high density was used to clearly observe melt flow patterns in the molten pool or in the rear and front part of a keyhole. It is observed that the underfilling degree of about 2 mm under the top surface of pure titanium plate was generated due to

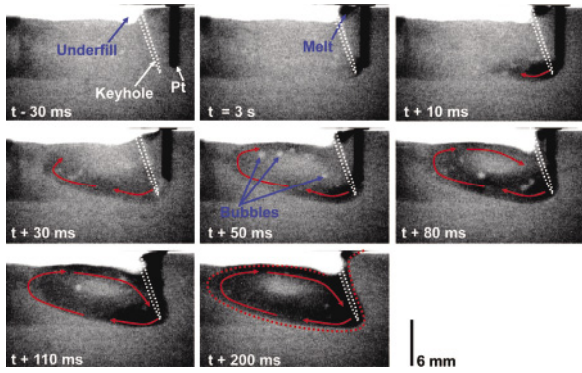


Fig. 7 Keyhole location and melt flows in molten pool during high power laser welding of thick plate of pure titanium, showing concavity or underfill on top surface, bubbles generation in molten pool and melt flow pattern observed by platinum (Pt) melting during laser welding.

spattering. Pt melting was first observed at the keyhole tip, and the melt flowed along the bottom of the molten pool from the keyhole tip to the rear part. Bubbles were also generated from the keyhole tip. The melt enriched in Pt and bubbles flew in the similar traces. Such typical melt flows in the molten pool during laser welding of Ti plate were the same as those of Type 304 austenitic stainless steel and aluminum alloys reported by Matsunawa, Katayama et al.^{18,9)}

Three-dimensional X-ray transmission in-situ observation of melt flows in the molten pool and spattering was performed during laser welding of pure titanium plate at 10 kW and 17 mm/s. The results of some melt flows are shown in three-dimensional display in **Fig. 8**. Here, the zero point indicates the center of the laser beam at its focal point. The location and the velocity of spatters were traced by tracking twenty WC (tungsten carbide) particles of 0.5 mm in sphere size in the molten metal. Two main flows were confirmed in the molten pool behind and in front of the keyhole. That is to say, the tracer particles flowed behind near the molten pool bottom from the keyhole tip, flowed upwards near the rear part of the molten pool, and then moved to the front near the surface of the molten pool. These flows were the same as the flows of Pt melting. On the other hand, some tracer particles near the surface in front of the keyhole flowed upwards and flew outside of the molten pool.

According to the calculation results of three-dimensional flows of tracer particles, the average velocity of the melt flow was 0.93 m/s in the keyhole tip, 0.28 m/s in the molten pool rear end and 0.58 m/s from the molten pool rear part to the keyhole tip. The average velocity of the whole molten pool was 0.57 m/s. On the other hand, molten metal flowed over the front wall of the keyhole and jumped out of the specimen surface at the average of 0.73 m/s and 0.92 m/s, respectively. Consequently, it was confirmed that melt flows near the front of the keyhole inlet were related to spatters formation.

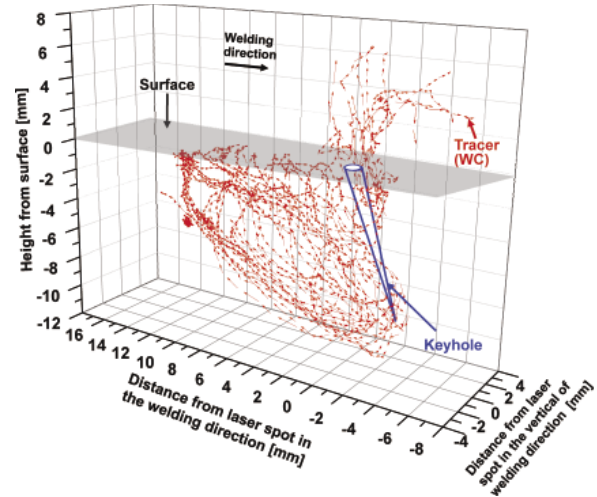
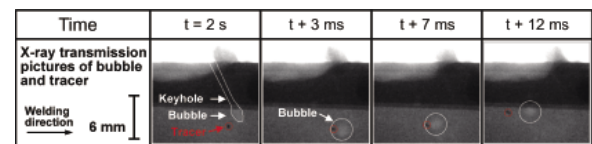
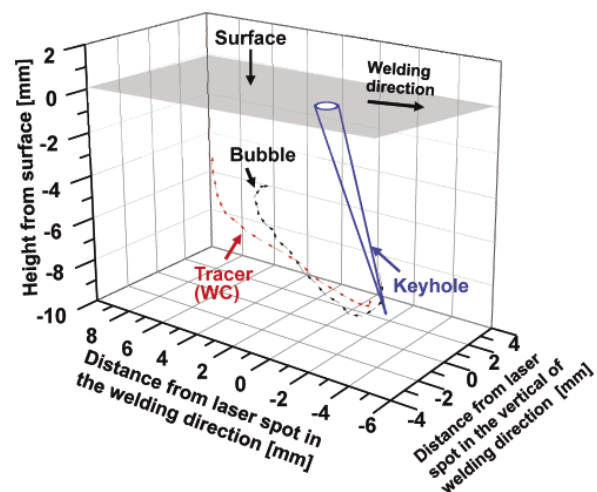


Fig. 8 Three-dimensional visualization of melt flows calculated from 20 tracers during laser welding of titanium plate at 10kW power and 17mm/s welding speed.

The movement velocity of a WC tracer particle was compared with that of bubbles generated from the keyhole tip in the molten pool. The micro-focused X-ray transmission in-situ observation photos and the three-dimensional display of the WC tracer and the bubble are shown in **Fig. 9**. A bubble of about 1.5 mm in diameter was broken away from the expanded tip of the keyhole, and flowed toward the rear part of the molten pool. The average velocities of the WC particle and the



(a) Micro-focused X-ray transmission images



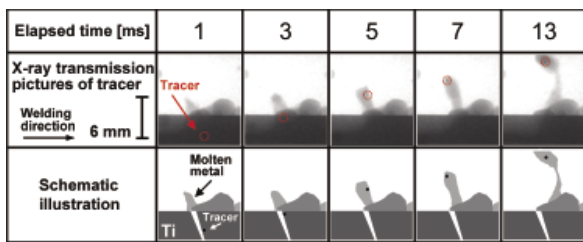
(b) Three-dimensional visualization of bubble behavior and WC trace from micro-focused and mini-focused X-ray transmission images

Fig. 9 Photos of WC tracer and bubble behavior during laser welding of titanium plate at 10 kW power and 17 mm/s welding speed.

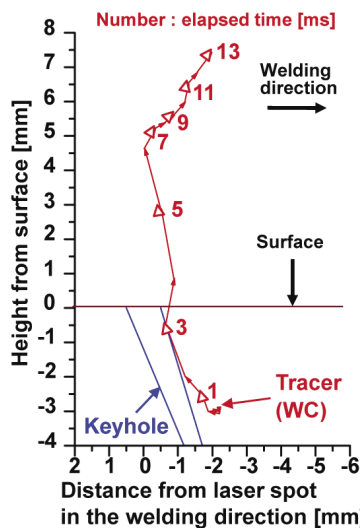
bubble were 0.64 m/s and 0.63 m/s, respectively, which were both almost the same velocity. Consequently, it is suggested that the melt flows along the centerline of the molten pool are by far faster than the welding speed, and that a WC particle and a bubble can be used as an example of melt flows in the molten pool.

3.3 X ray transmission in-situ observation results of relationship between melt flow and spatter

Trajectory and the velocity of the tracer particle were measured and investigated in further detail in relation to the generation and formation of a spatter. A typical formation mechanism from some melt to a spatter is summarized in Fig. 10. A series of micro-focused



(a) Micro-focused X-ray transmission in-situ observation result and schematic illustration of tracer and elongated melt with elapsed time



(b) Two-dimensional trajectory of tracer (WC)

| | | | | | | | |
|--------------------------|------|------|------|------|------|------|------|
| Elapsed time [ms] | 1 | 2 | 3 | 4 | 5 | 6 | 7 |
| Velocity of tracer [m/s] | 0.53 | 0.70 | 1.63 | 1.65 | 2.10 | 1.82 | 1.28 |
| Elapsed time [ms] | 8 | 9 | 10 | 11 | 12 | 13 | |
| Velocity of tracer [m/s] | 0.74 | 0.37 | 0.54 | 0.56 | 0.99 | 0.81 | |

(c) Velocity of tracer (WC) with elapsed time

Fig.10 Summary of characteristics of spattering in laser welding of titanium plate after 2 seconds from start of laser irradiation.

X-ray transmission in- situ observation photos shows a two-dimensional trajectory of a tracer particle which was ejected together with a melt droplet resulting in a spatter. The table (c) in Fig. 10 also indicates tracer velocity at various points in time.

The results show that the tracer near the surface of the specimen, originally located ahead of the keyhole, first started to move toward the top surface of the specimen along the front wall of a keyhole at a velocity ranging from 0.53 m/s to 0.7 m/s. Then, as it approached the surface, it was accelerated and eventually reached a velocity of about 1.6 m/s. The tracer moved above the top surface of the specimen, and the velocity was kept 1.65 m/s. At the height of more than 2 mm above the surface, the velocity increased to the maximum of 2.1 m/s. The tracer was still contained in the melt elongated from the molten pool and approached the tip of the elongated molten metal. The melt including a tracer particle near the tip was ejected away as a spatter. It was found that the melt continued an upward one-way flow to form the elongated shape, and the tip part was ejected and finally torn off, resulting in a spatter.

It was also observed that the elongated melt does not always lead to a spatter, but may be affected by gas streams induced by plumes ejection from the keyhole inlet. The results are shown in Fig. 11. A tracer particle located originally at the depth of 3.5 mm below the surface was accelerated along the keyhole wall from 0.67 m/s to 1.37 m/s. At a height of 2 mm above the specimen surface, it eventually reached the maximum velocity of 1.48 m/s. However, the tracer did not accelerate continuously but instead decelerated to a speed of 0.57 m/s, and then returned near the keyhole inlet. The existence of returned melt flows ahead of the keyhole inlet, leading to no spattering, was confirmed. It occurred in the case of some difference in the direction between plume ejection and melt elongation and the suppression of upward velocities of melt flows.

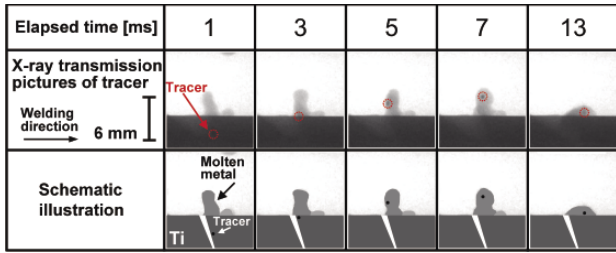
4. Conclusion

This study was undertaken to clarify melt flows and spatter formation mechanisms from the molten pool resulting in the formation of an underfilled bead during 10 kW laser welding of pure titanium. The results are as follows.

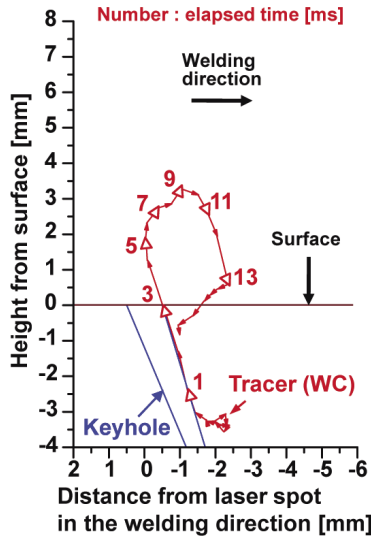
1) Spatter formation and welding speed;

- (i) The surface appearances show that the weld beads with spatters were formed at all welding speeds. At the lower welding speed of 17 and 50 mm/s, the spatters exceeding 1 mm in diameter were formed.
- (ii) At the lower speed of 17 and 50 mm/s, about 80 % of the elongated melts were generated from the front or sides of a keyhole. On the one hand, at the speed of 300 mm/s, about 80 % spatters were ejected from the molten pool just behind a keyhole.
- (iii) Spatters of more than 1 mm in diameter were formed at a lower welding speed.

Fundamental Study for Relationship of Melt Flows and Spatters in High Power Laser Welding of Pure Titanium



(a) Micro-focused X-ray transmission in-situ observation result and schematic illustration of tracer and elongated melt with elapsed time



(b) Two-dimensional trajectory of tracer (WC)

| | | | | | | | |
|--------------------------|------|------|------|------|------|------|------|
| Elapsed time [ms] | 1 | 2 | 3 | 4 | 5 | 6 | 7 |
| Velocity of tracer [m/s] | 0.67 | 1.18 | 1.37 | 1.48 | 0.57 | 0.57 | 0.55 |
| Elapsed time [ms] | 8 | 9 | 10 | 11 | 12 | 13 | |
| Velocity of tracer [m/s] | 0.51 | 0.53 | 0.54 | 0.71 | 0.70 | 1.39 | |

(c) Velocity of tracer (WC) with elapsed time

Fig. 11 Summary of characteristics of no spattering in laser welding of titanium plate after 0.5 seconds from start of laser irradiation.

2) Spatters formation and melt flows from X-ray transmission in-situ observations;

(i) The average flow velocity of melts rising along the front wall of a keyhole and jumping up from the specimen surface were 0.73 m/s and 0.92 m/s, respectively. It was found that melt flows resulting in spatters in front of the keyhole inlet were higher than the velocity of the whole molten pool.

(ii) WC (tungsten carbide) tracers demonstrated that the melt flows rose along the keyhole wall at a velocity of less than 0.6 m/s and then were accelerated to 2.1 m/s above the keyhole inlet.

(iii) The melt continued a one-way flow to form the elongated shape, and a tip part of the elongated melt was

torn off, resulting in a spatter.

(iv) In the case of no spattering, although the melt was elongated upward above the top surface, a circulatory melt flow occurred toward the keyhole inlet.

Acknowledgements

This work was partly supported by KAKENHI 25289240. The authors would like to thank Mr. Masami Mizutani, Technical Officer of JWRI, Osaka University, for discussion.

References

- 1) S. Li, G. Chen, S. Katayama and Y. Zhang, "Relationship between spatter formation and dynamic molten pool during high-power deep-penetration laser welding," *Appl. Surf. Sci.*, 303, 481-488 (2014).
- 2) M. J. Zhang, G. Y. Chen, Y. Zhou, S. C. Li and H. Deng, "Observation of spatter formation mechanisms in high-power fiber laser welding of thick plate," *Appl. Surf. Sci.*, 280, 868-875 (2013).
- 3) A. Heider, J. Sollinger, F. Abt, M. Boley, R. Weber and T. Graf, "High-speed X-Ray analysis of spatter formation in laser welding of copper," *Physics Procedia*. 41, 112-118 (2013).
- 4) M. Schweier, J.F. Heins, M. W. Haubold and M. F. Zaeh, "Spatter formation in laser welding with beam oscillation," *Physics Procedia*. 41, 20-30(2013).
- 5) A. F. H. Kaplan and J. Powell, "Spatter in laser welding," *J. Laser. Appl.* 23, 032005-1-7(2011).
- 6) Y. Kawahito, M. Mizutani, S. Katayama, "High quality welding of stainless steel with 10 kW high power fibre laser," *Sci. Technol. Weld. Join.*, 14, 288-294(2009).
- 7) K. Kamimuki, T. Inoue, K. Yasuda, M. Muro, T. Nakabayashi, and A. Matsunawa, "Prevention of welding defect by side gas flow and its monitoring method in continuous wave Nd:YAG laser welding," *J. Laser. Appl.*, 14, 136-145(2002).
- 8) A. Matsunawa, J. D. Kim, N. Seto, M. Mizutani, S. Katayama, "Dynamics of keyhole and molten pool in laser welding," *J. Laser. Appl.* 10, 247-254(1998).
- 9) S. Katayama, Y. Kobayashi, M. Mizutani, A. Matsunawa, "Effect of vacuum on penetration and defects in laser welding," *J. Laser. Appl.* 13, 187-192(2001).